ELSEVIER

Diamond and Related Materials 9 (2000) 446–451

DIAMOND AND RELATED MATERIALS

www.elsevier.com/locate/diamond

Evolution of thermoelastic strain and dislocation density during sublimation growth of silicon carbide

I.A. Zhmakin [a], A.V. Kulik [a], S.Yu. Karpov [a], S.E. Demina [b], M.S. Ramm [b,*], Yu.N. Makarov [c]

[a] *Soft-Impact Ltd., PO Box 33, 194156 St. Petersburg, Russia*
[b] *A.F. Ioffe Physical Technical Institute, Russian Academy of Sciences, Polytechnicheskaya 26, 194021 St. Petersburg, Russia*
[c] *Fluid Mechanics Department, University of Erlangen-Nürnberg, Cauerstrasse 4, D-91058 Erlangen, Germany*

Abstract

The evolution of crystallization front and growth conditions during sublimation growth of SiC bulk crystal is studied using a coupled heat and mass transport two-dimensional model. It is shown, in particular, that movement of the inductor coil used for heating of the growth crucible modifies the temperature profile at the growth surface but can have no remarkable effect on the growth rate.

Anisotropic elasticity theory and a semi-empirical model of dislocation generation are applied for a detailed analysis of thermoelastic strain and dislocation density evolution during SiC bulk crystal growth. An important effect of a method of SiC seed attachment to the holder is revealed by modeling. It is shown that under optimal attachment, the maximum dislocation density is concentrated near the crystallization front at the periphery of the crystal. The region of high dislocation density expands with enlargement of the crystal. © 2000 Elsevier Science S.A. All rights reserved.

Keywords: Bulk crystal; Dislocations; Physical vapor deposition; SiC; Thermoelastic strain

1. Introduction

The growth of high-quality bulk SiC crystals suitable for substrate fabrication is a key point for further development of high-temperature and high-power electronics. Nowadays, an insufficient crystal quality is commonly attributed to a high density of dislocations and micropipes generated during SiC growth. A close correlation between dislocations and micropipe formation has been revealed in several papers [1–3]. In turn, the generation of dislocations is known to depend significantly on the thermoelastic strain induced by the non-uniform temperature field inside the growth crucible.

Generally, thermoelastic strain arising in the SiC crystal is affected by the temperature distribution in the crucible, shape of the crystal, method of attachment used for seed fixation to a holder, adhesion of the crystal to the crucible walls, existence and location of wall deposits, etc. Most of these factors change during the growth of SiC crystals. Therefore, to analyze the role of thermoelastic strain, one should trace the evolution of the crystal and growth conditions at every stage of the growth process.

In this paper, we apply the coupled two-dimensional model of heat and mass transfer proposed in Refs. [4,5] to simulate the growth of the bulk SiC crystal by the sublimation technique. Using the computed temperature field and shape of the crystal, we analyze the dynamics of thermoelastic strain at different stages of growth. The distribution of dislocations generated due to thermoelastic stress relaxation is obtained using a semi-empirical approach [6]. Special attention is paid to the effects of the seed attachment to the holder.

2. Simulation of bulk crystal growth

Consider an axisymmetrical inductively heated growth system described earlier in Ref. [5]. Transport of the major gas species (Si, Si_2C, SiC_2 and inert gas — Ar) is simulated using a set of coupled equations for gas mixture density, momentum, energy and mass fractions of the reactive species. Both conductive and radia-

* Corresponding author. Fax: +7-812-326-6194.
E-mail address: ramm@model.ioffe.rssi.ru (M.S. Ramm)

0925-9635/00/$ - see front matter © 2000 Elsevier Science S.A. All rights reserved.
PII: S0925-9635(99)00307-6

tive mechanisms of heat transfer are taken into account to compute the temperature distribution in the growth system. Diffusion, convection and thermo-diffusion are considered as the main mechanisms of mass transport. These processes are involved in the model to predict the distribution of species concentrations in the growth crucible, growth rate, V^{cr}, for every point of the crystallization front and sublimation rate, V^{src}, at the surface of the SiC powder used as a material source. The Navier–Stokes equations reduced for low-Mach-number multi-component flows [7] are supplemented by a set of boundary conditions accounting for heterogeneous chemical reactions at various gas–solid interfaces (for more detail, see Ref. [4,8]).

Evolution of the SiC crystal shape and of the temperature field is simulated using a quasi-steady-state concept, which implies that the transient time of all the processes occurring in the growth system (inductor movement, crystal growth, source sublimation, temperature field variation, etc.) is much less than the total duration of the growth run. This allows us to replace the original growth process with the slow change of parameters by a number of steady-state growth steps where only the variation of the growth conditions from step to step is taken into account. In particular, the position of the inductor coil at every step is calculated using the time-dependent inductor velocity specified by growers. To predict the evolution of the shape of the crystallization front and powder charge surface, the values of V^{cr} and V^{src} obtained at the previous growth step are used.

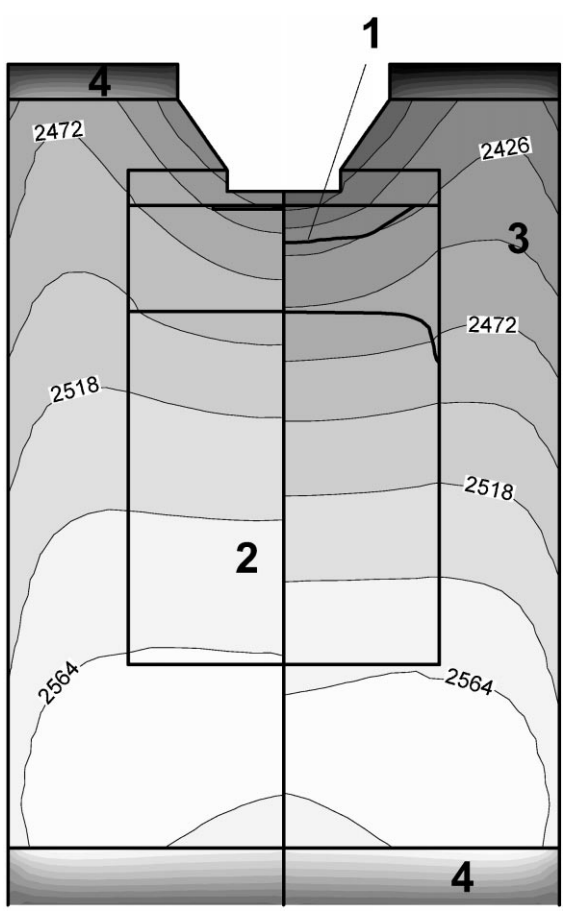

Fig. 1. Two-dimensional temperature distribution in the crucible at the initial stage of sublimation process (left) and after 20 h of growth (right). The inductor coil shifts during SiC growth. 1: crystallization front; 2: SiC powder charge; 3: tantalum growth crucible; 4: graphite thermal insulation.

Fig. 1 shows the two-dimensional temperature field in the growth crucible at the beginning ($t=0$) and end ($t=20$ h) of a growth run computed for the case of driven inductor. It can be seen that the temperature field is modified during growth, first of all, in the upper part of the crucible. This effect is related to the replacement of the inductor coil and the enlargement of the SiC crystal.

Temporal variations of temperature and of the growth rate computed for the cases of driven (solid lines) and immobile (dashed lines) inductor coil are plotted in Fig. 2. As the inductor coil movement has a significant effect on temperature evolution, the growth rate is found to be practically insensitive to the coil position. The maximum growth rate reached at the edge of SiC crystal tends to decrease significantly with time. The growth rate at the center of the crystal is lower than at the edge of the crystal but remains almost constant during growth. This different behavior of the growth rate at the center and at the edge of the crystal leads, first, to smoothing of the initially concave shape of the crystal and then to a transition of the shape from concave to convex one (see also Fig. 3).

3. Thermoelastic strain in the SiC crystal

Normally, the direction of SiC growth generally corresponds to the hexagonal [0001] axis of the crystal. As the temperature field is axisymmetrical, the thermoelastic strain should be isotropic with respect to rotations over the hexagonal axis. This means that the thermoelastic strain can be computed using a two-dimensional approach where elementary displacements in the crystal caused by deformation occur only in radial and axial directions.

Let the crystal be free of strain at the uniform temperature, T_{ref}. The temperature distribution during growth $T(r, z)$ can be obtained by coupled modeling of heat and mass transfer in the growth system (see Section 2). In this case, Hooke's law can be written as

$$\begin{pmatrix} \sigma_{rr} \\ \sigma_{\phi\phi} \\ \sigma_{zz} \\ \sigma_{rz} \end{pmatrix} = \begin{pmatrix} c_{11} & c_{12} & c_{13} & 0 \\ c_{12} & c_{11} & c_{13} & 0 \\ c_{13} & c_{13} & c_{33} & 0 \\ 0 & 0 & 0 & c_{44} \end{pmatrix} \begin{pmatrix} \epsilon_{rr} - \alpha_{\perp}(T - T_{ref}) \\ \epsilon_{\phi\phi} - \alpha_{\perp}(T - T_{ref}) \\ \epsilon_{zz} - \alpha_{\parallel}(T - T_{ref}) \\ \epsilon_{rz} \end{pmatrix}, \quad (1)$$

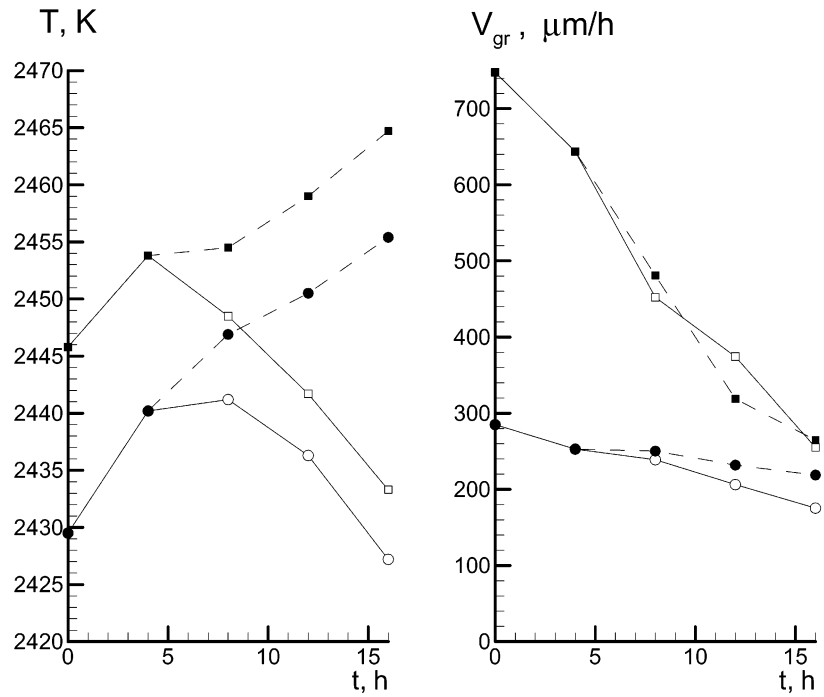

Fig. 2. Evolution of the temperature (left) and of the growth rate (right) at the center (circles) and at the periphery (squares) of the crystal. Solid (open symbols) and dashed (solid symbols) lines correspond to the mobile and immobile inductor coil, respectively.

where c_{ij} denotes the elastic constants written in Voigt notation, $\alpha_{\parallel}$ and $\alpha_{\perp}$ are the thermal expansion coefficients along, and perpendicular to, the [0001] axis, and ϵ_{rr}, $\epsilon_{\phi\phi}$, ϵ_{zz} and ϵ_{rz} are the components of the deformation tensor

$$\epsilon_{rr} = \frac{\partial v}{\partial r},\ \epsilon_{\phi\phi} = \frac{v}{r},\ \epsilon_{zz} = \frac{\partial u}{\partial z},\ \epsilon_{rz} = \frac{\partial u}{\partial r} + \frac{\partial v}{\partial z}, \tag{2}$$

where u and v are the axial and radial components of the displacement field, respectively.

Substituting Eqs. (1) and (2) into the equation of static equilibrium, we obtain a set of partial differential equations for the components of the displacement vector u and v.

The boundary conditions for these equations imply zero stress components normal to the free surface of the crystal. Three types of boundary conditions are used for the surfaces where the seed is attached to the holder and where the crystal comes into contact with the upper wall of the crucible. All of them correspond to different methods of attachment:

(A) Rigid attachment: the SiC seed/crystal is rigidly bonded with the holder/upper wall of the crucible. In this case both components of displacement vector are suggested to be equal zero at the attachment surface.

(B) Pillow attachment: the seed/crystal and the holder/upper wall of the crucible are interspersed with a thin layer of a special plastic material allowing free movement of the seed/crystal along the attachment surface. In this case the axial components of displacement vector as well as the tangential components of the stress tensor are assumed to be equal zero.

(C) Free surface: such boundary conditions should be used if the plastic interlayer between the seed/crystal and the holder/upper wall of the crucible allows relaxation of not only tangential but also normal components of the stress tensor at the attachment surface.

4. Dislocation formation due to thermoelastic strain

Generally, to study dislocation dynamics, a kinetic approach needs to be used, accounting for dislocation threading from the seed to the crystal, nucleation and evolution of dislocation loops, multiplication and coagulation of the dislocation, their slipping due to strain forces, etc. However, taking into account high temperatures of SiC growth, we assume that strain relaxation caused by plasticity effects occurs inside the crystal rapidly compared to the overall time of crystal growing.

To estimate the distribution of dislocation density, we apply the approach proposed in Ref. [6] for III–V compounds. According to Ref. [6], in every point of the crystal, there is full relaxation of the thermoeleastic stress exceeding a critical value, σ_{th}, known as the threshold of plasticity. For III–V compounds, 12 components of the stress tensor corresponding to four slipping

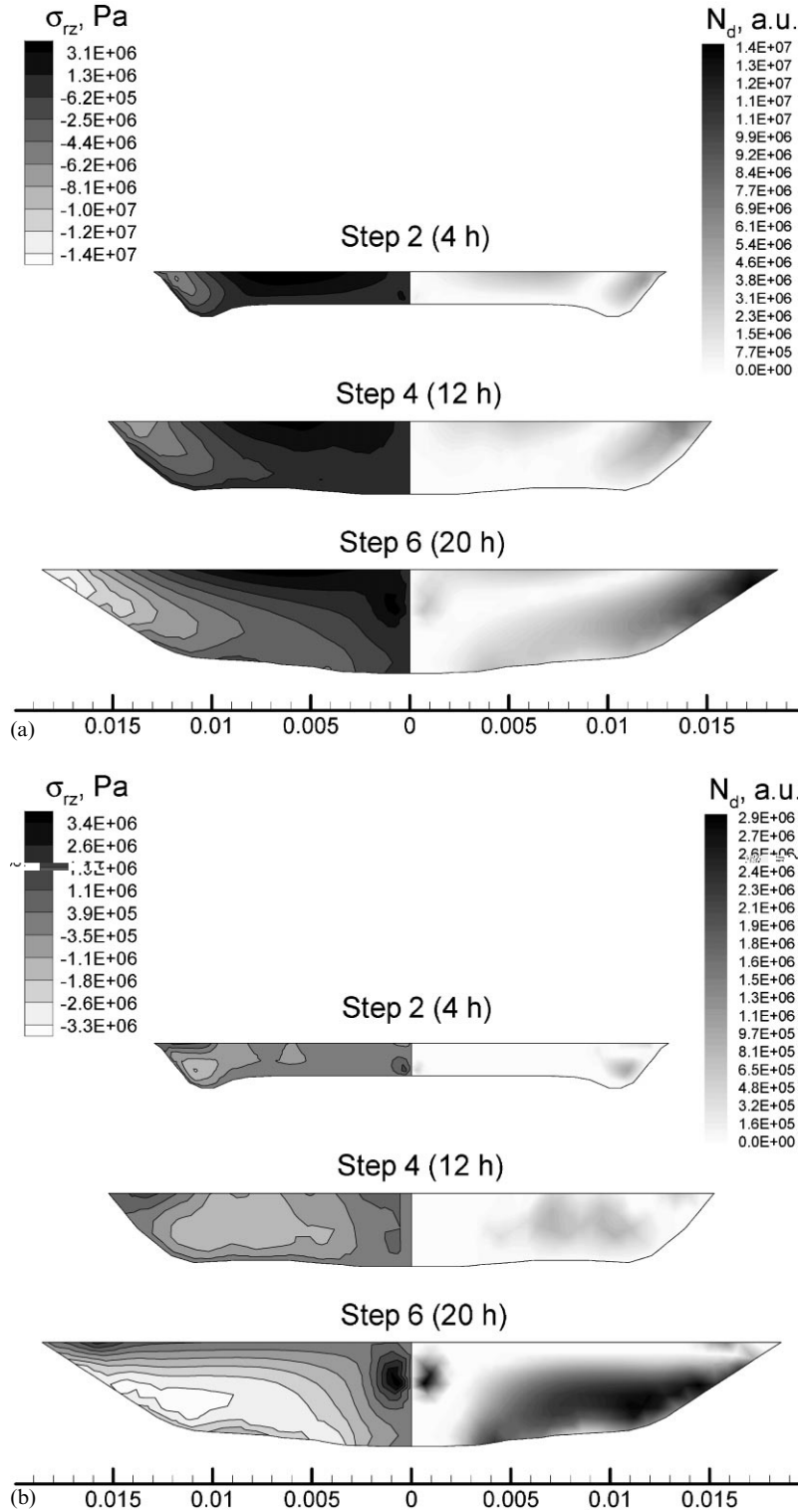

Fig. 3. Evolution of the stress component, σ_{rz}, and dimensionless dislocation density, N_d, in the growing crystal. (A) Rigid attachment; (B) pillow attachment; (C) stress-free attachment of the seed to the holder (see Section 3).

planes (of the (111) type) and three gliding directions (of the [110] type) are usually selected for comparison. In the case of α-SiC, the main slipping plain is the (0001) plain. Due to the isotropy of the crystal with respect to rotations over the hexagonal axis, there are only two independent directions related to dislocation gliding. For each of them, the stress component responsible for gliding of dislocations is σ_{rz}. Therefore, according

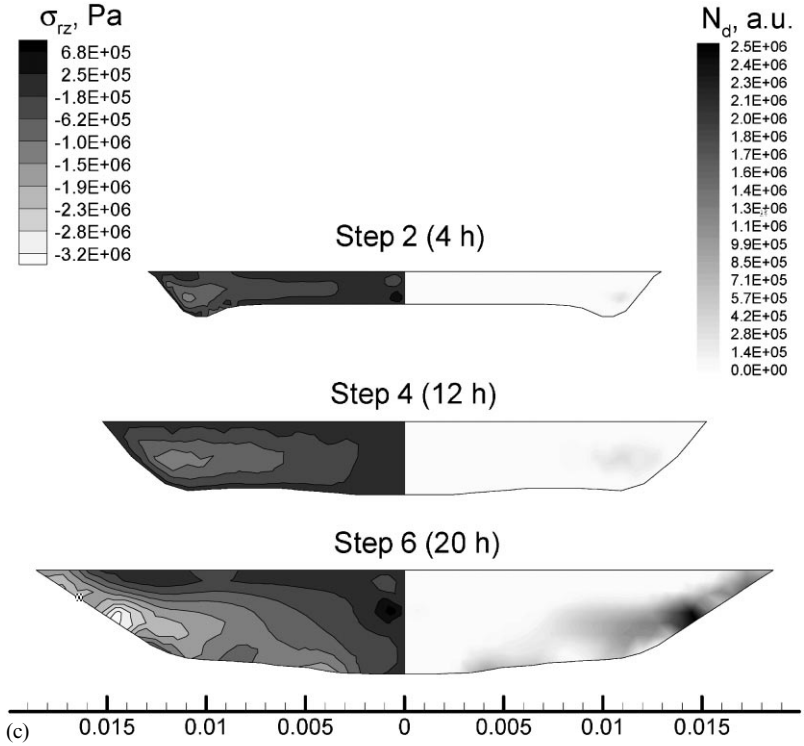

Fig. 3. (*continued*)

to the approach in Ref. [6], the dislocation density, N_d, should be proportional to the value $|\sigma_{rz}-\sigma_{th}|$.

Fig. 3 shows the evolution of the stress component, σ_{rz} (left), and of the dislocation density, N_d (right), for different types of seed attachment. Fig. 3a, b and c are obtained using the boundary conditions A, B and C, respectively (see Section 3).

It can be seen from Fig. 3a that the highest stress is generated in the crystal rigidly attached to the holder (boundary conditions A). In this case, the maximum dislocation density is located in two separate zones. The first is adjacent to the attachment surface. Generation of strain in this zone originates from the difference in thermal expansion coefficients of the seed and of the holder. It is interesting that the dislocation density here varies weakly with time. The second zone of higher stress is observed at the periphery of the SiC crystal. In contrast to the first zone, the dislocation density in the second zone rises significantly with crystal growth. Also, the region of high dislocation density gradually expands during growth.

The pillow attachment (boundary conditions B) and stress-free attachment (boundary conditions C) provide a similar shear stress and generated dislocation density. The dislocation density is about five times lower than that generated in the case of rigid attachment of the seed. Fig. 3b and c show that both stress and dislocations are concentrated near the crystallization front at the periphery of the crystal. The highly defective zone develops gradually with time expanding in both radial and axial directions.

5. Conclusion

Using the coupled model of heat and mass transport [5], we simulate evolution of the crystallization front and of the growth conditions during sublimation growth of SiC bulk crystal. It is shown that movement of the inductor coil used for heating of the crucible influences the temperature profile at the growth surface but under definite conditions has no remarkable effect on the growth rate.

We apply the anisotropic elasticity theory and semi-empirical approach of Ref. [6] for a detailed analysis of thermoelastic strain and dislocation density evolution during SiC bulk crystal growth. An important effect of a method of seed attachment to the holder on the dislocation density is revealed for the first time. It is shown that under optimal attachment, the maximum dislocation density is concentrated near the crystallization front at the periphery of the crystal. The region of high dislocation density expands with enlargement of the crystal.

In combination with mass and heat transport modeling, analysis of the thermoelastic strain and dislocation density is a powerful tool for optimization of growth

conditions intended to obtain high-quality bulk SiC crystals.

References

[1] R.G. Verenchikova, E.E. Goncharov, G.A. Lomakina, E.N. Mokhov, M.G. Ramm, A.D. Roenkov, G.G. Ryabova, A.S. Tregubova, 6th conference on growth and synthesis of semiconductor crystals and films, in: Book of Abstracts, Novosibirsk Vol. 2 (1982) 158, in Russian.

[2] A.S. Tregubova, E.N. Mokhov, A.D. Roenkov, I.L. Shulpina, A.V. Naumov, M.G. Ramm, 3rd workshop, physics and technology of wide band gap semiconductors, in: Book of Abstracts, Makhachkala (1986) 85, in Russian.

[3] R.H. Ma, Q.-S. Chen, H. Zhang, V. Prasad, C.M. Balkas, N.K. Yushin, in: ACCGE-11, Abstracts (1999) 35.

[4] M.S. Ramm, E.N. Mokhov, S.E. Demina, M.G. Ramm, A.D. Roenkov, Yu.A. Vodakov, A.S. Segal, A.N. Vorob'ev, S.Yu. Karpov, A.V. Kulik, Yu.N. Makarov, Mater. Sci. Eng. B 61–62 (1999) 107.

[5] S.Yu. Karpov, A.V. Kulik, I.A. Zhmakin, Yu.N. Makarov, E.N. Mokhov, M.G. Ramm, M.S. Ramm, A.D. Roenkov, Yu.A. Vodakov, J. Cryst. Growth (2000) in press.

[6] A.S. Jordan, R. Caruso, A.R. VonNeida, J.W. Nielsen, J. Appl. Phys. 52 (5) (1981) 3331.

[7] Yu.N. Makarov, A.I. Zhmakin, J. Cryst. Growth 94 (1989) 537.

[8] Yu.E. Egorov, A.O. Galyukov, S.G. Gurevich, Yu.N. Makarov, E.N. Mokhov, M.G. Ramm, M.S. Ramm, A.D. Roenkov, A.S. Segal, Yu.A. Vodakov, A.N. Vorob'ev, A.I. Zhmakin, Mater. Sci. Forum 264–268 (1998) 61.